Dependence of Semiconducting Materials on Temperature and Bias Voltage With NPN Transistors

Syed Murtaza Husain
PHY 353L Modern Laboratory
Department of Physics
The University of Texas at Austin
Austin, TX 78712, USA

November 9, 2025

Abstract

We investigate the characteristics of semiconductor devices through measurement and analysis of their I-V behavior under varying temperature and voltage bias conditions. Using the Ebers–Moll model, we performed exponential fits to transistor data to calculate the Boltzmann constant and the saturation current. The measured Boltzmann constants for silicon and germanium transistors were found to be on the order of $(1.4\text{–}1.7) \times 10^{-23}$ J/K, which agrees with the accepted value of 1.380649×10^{-23} J/K. The average saturation current we found across all transistor runs was determined to be $(6.07 \pm 2.06) \times 10^{-9}$ A, which aligns with expected nanoamp-scale leakage currents in silicon junctions. We go beyond the lab manual to analyze LED data using both the avalanche and Zener breakdown models. The avalanche fit produced a higher R^2 value of 0.8727 compared to the Zener fit's R^2 of 0.5632, indicating that avalanche breakdown dominates at $V_{\text{BR}} = 3.3 \pm 0.05$ V. Finally, we analyzed op-amp diode characteristics by fitting the Ebers–Moll model and finding an average saturation current of $(1.55 \pm 0.047) \times 10^{-9}$ A with ideality factors ranging from $n = 7.6$ to $n = 8.1$, demonstrating strong exponential behavior as expected but significant deviation from ideal diode behavior due to internal junction complexity and noise.

1 Introduction

1.1 Physics Motivation

Semiconductors are ubiqetous and extremely important materials in modern electronics. Their properties of conductivity can be controlled by temperature, illumination, and doping, allowing them to act as either conductors or insulators dynamically. Semiconductors are the fundamental building blocks of diodes, transistors, and integrated circuits like op-amps. At the microscopic level, semiconductors are materials whose valence and conduction bands are separated by an energy gap E_g that's on the order of 1 eV [12].

Thomas Johann Seebeck and Michael Faraday were some of the first to notice the special conducting properties of semiconductors in the 1820s-1830s. Faraday heated silver sulfide samples and found that the resistance of the heated sample was less than it was at room temperature. The useful properties of these materials would be used in electronics starting in 1874 when Karl Ferdinand Braun created an AC-DC rectifier using semiconductor properties. Over the next century, triode vacuum tubes, transistors, diodes, and many of the useful integrated circuits depending on these components were born. Many of these were pioneered by the famous AT&T Bell laboratory [11]. Near the 1950s, the creation of these components shifted from utilizing germanium, which at the time was used for its high level of electrical response, to silicon, which had a higher bandgap but was also less expensive.

Semiconductors are often 'doped,' which is the process of adding a small amount of donor atoms consisting of different elements to pure semiconductor materials to fine tune their response to current. Often, these doped substances are either 'p-type,' which involve injecting atoms that have a lack of electrons compared to the semicon-

ductor material, or 'n-type,' which have an excess of electrons. This results in p-type materials halting current flow, and n-type materials encouraging it [7]. Using both together creates p-n junctions, which is the basis for many electronic components such as the diode and transistor, as it halts current flow originating in the p direction while letting current through the n direction undisturbed.

Understanding semiconductor current–voltage characteristics, carrier transport, and band structure is extremely important in order to gain a better understanding of solid-state physics and practical applications in electronics and computing.

1.2 Theoretical Background

1.2.1 Ebers-Moll, Boltzmann Constant and Saturation Current

The Boltzmann constant, k_B, which is a fundamental constant that is used in many areas of physics, can be determined from the temperature dependence of a semiconductor's forward current in the exponential region of its I–V curve. This is done using the Ebers-Moll equation, which uses an ideal diode to describe the base-emitter junction current [9]:

$$I = I_s\left(e^{\frac{eV}{nk_BT}} - 1\right) \tag{1}$$

where I_s is the saturation current, e is electron charge, V is the applied voltage, T is the junction temperature, and n is the ideality factor [2].

Taking the natural log of (1) for the forward-bias region ($eV \gg nk_BT$) gives us:

$$\ln I = \ln I_s + \frac{eV}{nk_BT}. \tag{2}$$

The fit $\ln I$ versus V gives us the slope:

$$k_B = \frac{e}{mTn} \tag{3}$$

In the ideal case ($n = 1$), k_B can be directly calculated from the measured slope at each temperature.

We can also use this to fit the saturation current I_s. By fitting $\ln I$ versus V_{BE} in the exponential region of the forward-bias curve we can find fits for the parameters:

$$m = \frac{e}{nk_BT}, \qquad \ln I_S = b$$

The intercept b is the natural log of the saturation current, from which

$$I_S = e^b$$

This constant represents the current due to leakage when the base–emitter voltage is zero.

1.2.2 NPN Transistors

Transistors, particularly bipolar junction transistors (BJTs), are one of the most important electronic components to be created using semiconducting materials. They act as amplifiers and switches by utilizing two p–n junctions to modulate current flow through a small base current or voltage, which outputs high current gain. Typical BJTs have three pins, a base, emitter, and collector. The transistors we utilize in this experiment will be NPN transistors, in which there is a central p-type region that can be saturated by applying voltage to the base, which causes the current from the collector to be able to move into the emitter. This results in the characteristic amplification that transistors are known for, as a small variation in base voltage can cause a large difference in current from the collector to the emitter [6]. Because of the semiconductor properties within the n and p regions of the transistor, this also means that very little current will leak through the transistoy when the base voltage is not saturated.

1.2.3 Silicon Transistors

Silicon is the currently most widely used semiconductor due to its stable oxide, abundant supply, and bandgap of approximately 1.12 eV at room temperature. Silicon BJTs exhibit have good stability across a large voltage and temperature range, meaning they are ideal for modern electronics. Silicon is usually doped with elements like phosphorus and arsenic to create n regions and boron to create p regions [14].

1.2.4 Germanium Transistors

Germanium transistors have a smaller bandgap of about 0.66 eV compared to silicon, which means they have lower forward voltage thresholds and higher leakage currents. This also affects the amount of electrons that can cross the gap due to thermal excitation, meaning germanium transistors are less stable at higher temperatures. Germanium transistors are usually doped with elements like antimony or arsenic to create n regions and gallium or

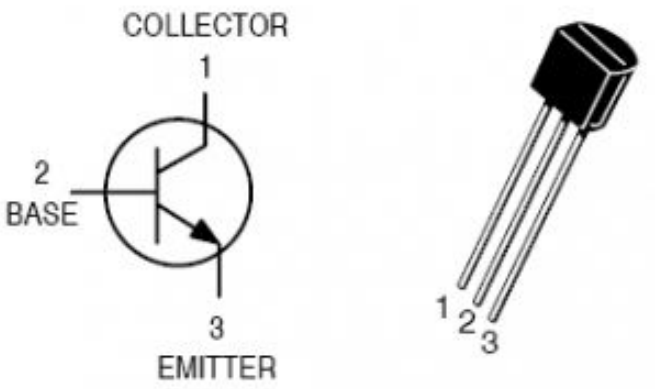

Figure 1: A diagram and image of a bipolar junction transistor (BJT) and the relevant pins. The voltage applied to the base fills an n-type region that causes amplification and large current flow from the collector to the emitter. Image sourced from [13].

boron to create p regions. Comparing silicon and germanium transistors can provide insight into how intrinsic material properties affect device characteristics and temperature dependence [2].

1.2.5 Light Emitting Diodes

Diodes are ubiqetous circuit components that allow current to flow in one orientation but block current from flowing through in the opposite direction. The way this is done is by having the forward biased direction have the n-type material carry charge into the p-type region so that current can flow [7]. In the reverse orientation, current is blocked by the p-type material before it is able to reach the n-type material. Light-emitting diodes (LEDs) are diodes that emit light at a specific frequency that is determined by the bandgap of the PN junction of the semiconductor material, with electrons losing energy and emitting photons within the semiconductor material [8].

While an ideal diode does not leak any current in the reverse-biased direction, real diodes still sometimes leak small amounts of current. At small reverse voltages, the leakage current I_{leak} is caused mostly by thermal generation in the p region and is approximately constant. As the reverse bias approaches what is known as the breakdown voltage V_{BR}, the current increases through two possible ways:

Zener Breakdown (happens at $V_{\text{BR}} \leq 5$ V): quantum-mechanical tunneling of electrons through the p barrier, producing an exponential result

$$I(V) = I_0\, e^{(V - V_{\text{BR}})/V_0} \tag{4}$$

Avalanche Breakdown (dominant at higher voltages): carrier impact ionization leading to a power-law behavior

$$I(V) = A\,(V - V_{\text{BR}})^n \tag{5}$$

where n describes the steepness of the avalanche [8][2].

Both of these can be applied to diodes exhibiting leakage to quantify which effect is more prominent at a given voltage for a given diode.

1.2.6 Operational Amplifiers

Operational amplifiers (op-amps) are widely used integrated circuits that consist of multiple transistor stages designed to provide high open-loop gain and differential input characteristics [2]. They convert the nonlinear behavior of transistors into linear amplification of input by the difference of the two inputs, known as the inverting and noninverting inputs. This is done by pulling from the rail voltages, which are positive and negative DC inputs given to the op-amp, and outputting a potential difference depending on the inputs using the rail voltages. A full diagram of an op-amp is shown in figure 2.

Op-amps have a saturation current which corresponds to the transistor stages that they are comprised of. Below the saturation current, the transistors will not turn on and the output will not appear. The output is qualitatively different from a transistor because of the linear amplification that the op-amp produces. When outputting current, the output I_{out} is proportional to the input voltage difference V_{in}:

$$I_{\text{out}} = \frac{V_{\text{in}}}{R_{\text{eq}}}$$

where $R_{\text{eq}}$is the feedback resistance. When the amplifier enters saturation, I_{out} approaches a maximum value determined by the rail voltage (it can't output more than it is being supplied) and internal transistor limits.

The current vs voltage of a p-n junction is given by the Ebers-Moll equation 1 [6] [12].

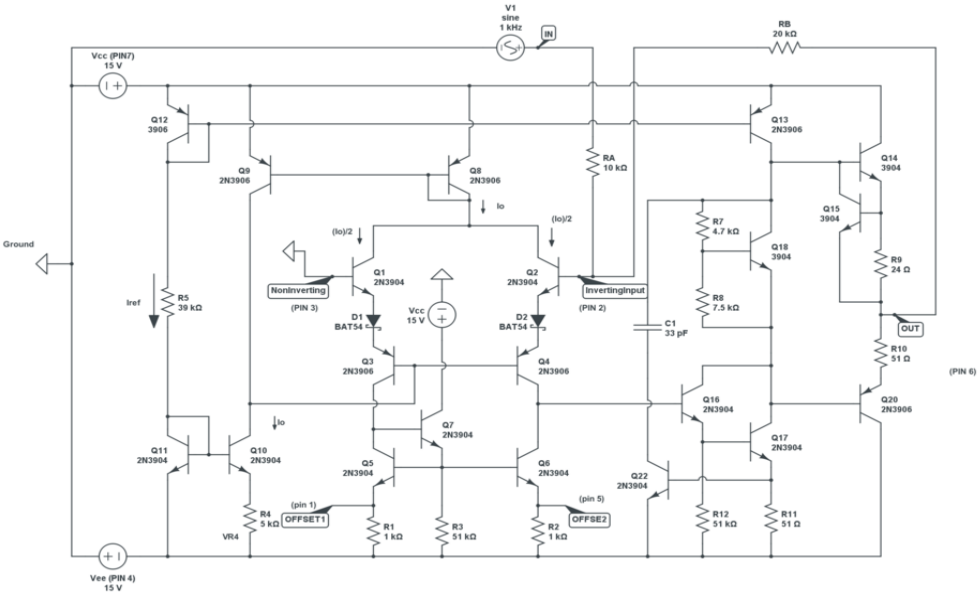

Figure 2: A full diagram of an operational amplifier (op-amp) integrated circuit. It is comprised of many transistor stages which make up a differential amplifier that is sent through a gain stage into the output. Image sourced from [1].

For moderate forward bias ($qV \gg nk_BT$), we can ignore the -1 term and obtain:

$$I \approx I_S\, e^{\frac{qV}{nk_BT}} \tag{6}$$

Taking the natural logarithm gives us:

$$\ln I = \ln I_S + \frac{qV}{nk_BT} \tag{7}$$

Which can be fit to data to tell us how the diodes in a particular op-amp behave.

1.3 Equipment Background

There are several important pieces of equipment utilized in this experiment, including the described transistors as well as a power resistor, picoammeter, thermocouple, NI digital acqusition module (DAQ), labview software, LED, and LM308 op-amp.

We utilize a Keithley 6485 picoammeter for high-precision current measurements. It is capable of measuring currents in the picoamp range with relatively low input bias and noise. Like any ammeter, the signal we want to measure must be run through the device directly [5].

Our thermocouple is a device that is a temperature sensor made of two distinct metal wires that have been joined together. Utilizing the Seebeck effect, in which temperature differences can be converted into electric potential differences, putitng the thermocouple in physical contact with the transistor or transistor plate can allow us to measure its temperature. The Seebeck effect states that the measured voltage from the thermocouple follows

$$S_1 - S_2 = \frac{\Delta V_{12}}{\Delta T_{12}} \tag{8}$$

where S_1, S_2 are the Seebeck coefficients of each material, ΔV_{12} is the difference in voltage between the two materials, and ΔT_{12} is the difference in temperature [10].

The NI USB-6346 DAQ [3] is very useful in this experiment to output varying or constant DC voltages from the analog output terminals, and read analog signals from the picoammeter or thermocouple. A labview program provided by the modern physics lab website provides an easy setup for performing this.

1.4 Our Approach

In this experiment, we will measure the current through the base-emitter junction of silicon and germanium transistors as a function of bias voltage and temperature and analyze the change in collector current. This will be done

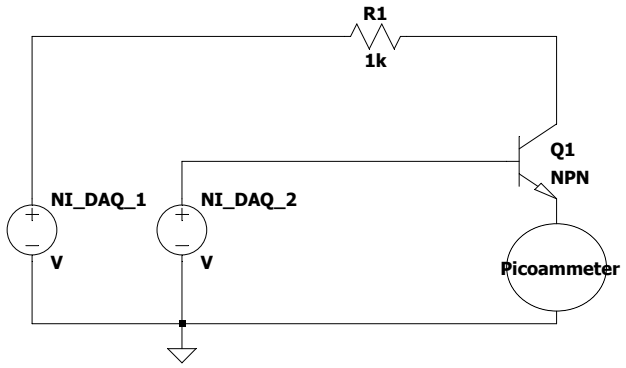

Figure 3: Circuit diagram to test the current through the base-emitter junction of the NPN transistor. The NI DAQ outputs a ramping DC voltage to the base to increase the base-emitter voltage and the collector current is measured using the Keithly picoammeter.

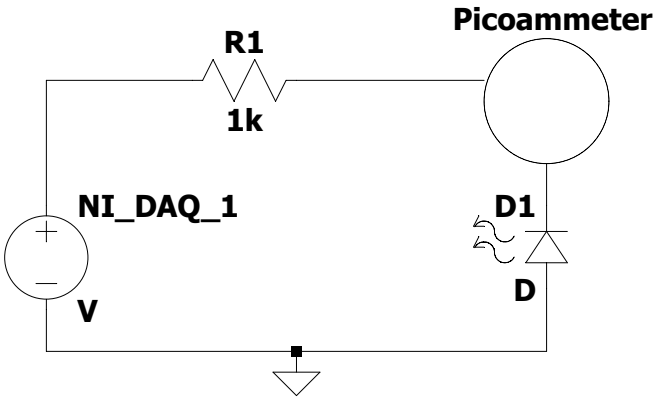

Figure 4: Circuit diagram used to test the semiconductor properties of LEDs. By running a ramping voltage through the NI DAQ, we are able to use the picoammeter to measure the current that leaks through the diode [2].

using a power resistor to dissipate heat onto the transistor plate, as well as submerging a transistor into a container filled with liquid nitrogen, that can cause the transistor to reach temperatures as low as 80 K. Furthermore, we go beyond the lab manual and apply similar analyses of the breakdown voltage of LEDs to characterize their semiconductor properties. Finally, we explore the saturation current of the op-amp IC and verify that semiconductor properties are present.

2 Experimental Setup

2.1 Apparatus

In this experiment, we have several unique setups. When measuring the current through the transistor, we use the setup shown in figure 3.

Additionally, we utilize the lab's pre-built apparatus, shown in figure 7, which involves convenient terminals to connect to the silicon and germanium transistors, as well as a power resistor on the bottom of the plate containing the transistors, which allows for easy heating of the components.

To test the semiconductor properties of op-amps and LEDs, we use the circuits shown in figures 4 5.

As a result of the current we measure while sweeping voltage across 3, we expect to see a rise consistent with the Ebers-Moll equation in the region where the transistor saturation has been satisfied and the output has not plateaued.

By utilizing the LED circuit in figure 4, we can analyze the current leakage across the p-region of the LED. We can use this data to quantify which effects account for this current leakage more effectively between equations 5 and 4.

The circuit in figure 5 utilizes a LM308 op-amp [1] to test the saturation voltage required for the IC to output current. We expect that when the DAW voltage rises above the saturation voltage, a linear response is outputted by the op-amp. By tying the output into the inverting input, we create a differential amplification scheme which draws more current to stabilize the potential between the inputs.

To measure the temperature dependence of the silicon transistor at very low temperatures, we use a transistor not attached to an apparatus like the one we use for the heated trials, and we submerge it in a vat of liquid nitrogen to measure the semiconductor properties at low temperature.

2.2 Data Collection

There were many trials of data taken with the transistors. The germanium and silicon transistors were both heated using the power resistor and the relationship between their voltage and current was recorded. The silicon transistor was also cooled in liquid nitrogen and the same properties were measured. All of the trial runs can be seen in the comprehensive table 1. An exmaple of a measurement taken from a silicon transistor under liquid

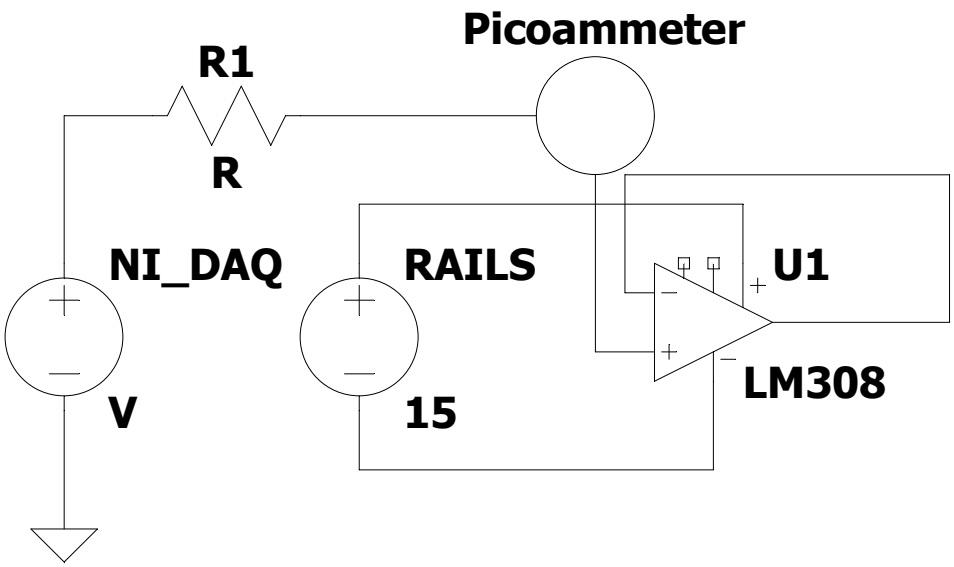

Figure 5: Circuit built to detect the semiconductor properties of an LM308 op-amp. The inverting input is tied to the output of the op-amp to create feedback, while the noninverting input has a ramping voltage fed to it through the ammeter. This allows the measurement of the voltage at which current starts to flow freely and exhibit Ohmic behavior, vs when the semiconducting band gap is not full [2].

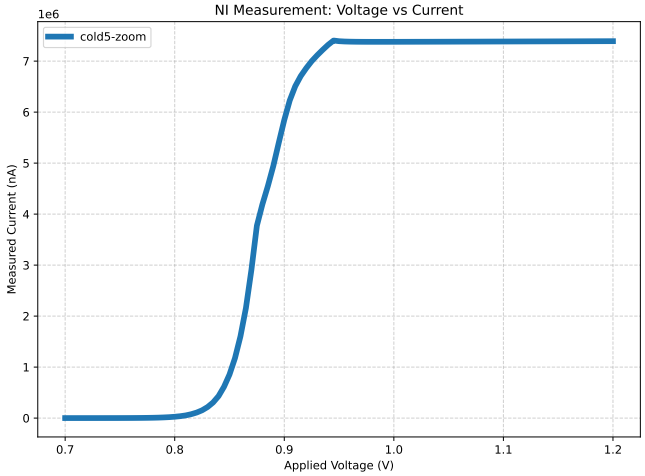

Figure 6: I-V curves for op-amp circuit shown in 3 across voltage sweeps done by using NI DAQ and labview. There is a clear region in which the p-region has not yet been saturated, and then a plateau in which the current does not increase.

nitrogen cooling is shown in figure 6.

In addition to these measurements, we take three measurements each of the diode and op-amp properties mentioned in sections 1.2.5 1.2.6 and shown in figures 4 5. These measurements are shown in 8 9.

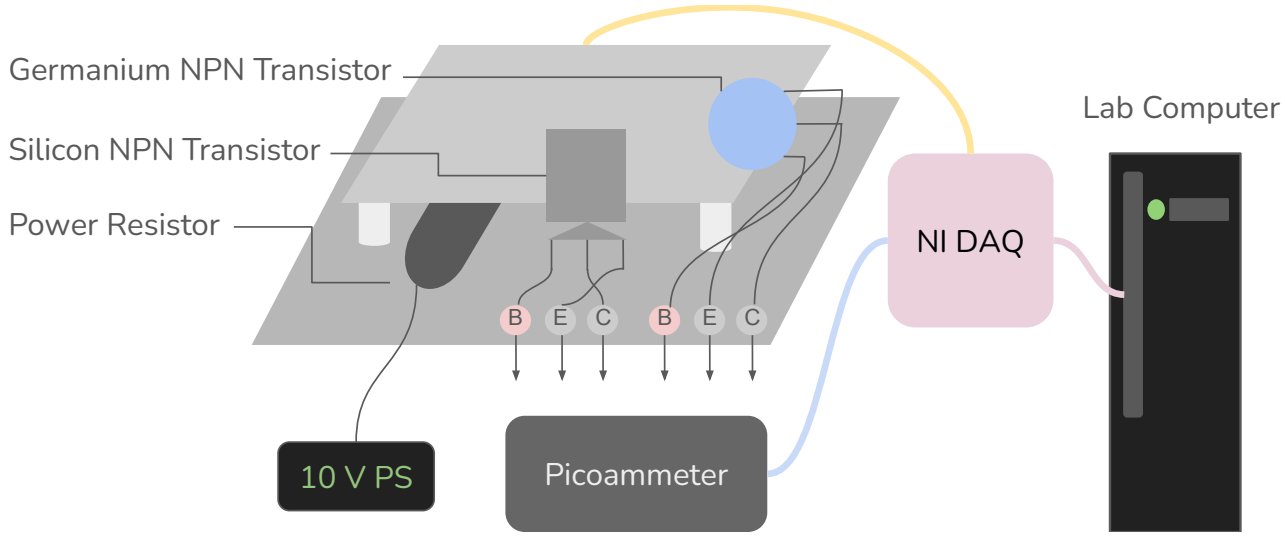

Figure 7: Silicon and germanium heating and I-V curve measurement apparatus. The wiring of each transistor is given by 3. The power resistor dissipates heat into the transistor holding plate, which affects the current detected through the picoammeter for a given voltage that is swept by the NI DAQ. All data is then recorded on the lab computer through labview.

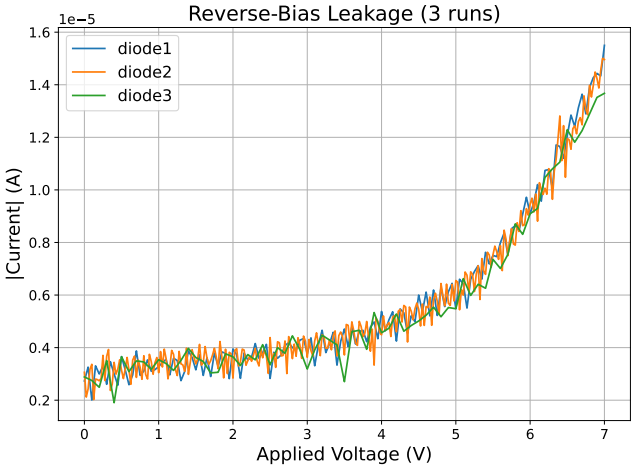

Figure 8: LED current leakage across 3 voltage sweeps done by using NI DAQ and labview. There is a small amount of current leakage, illustrating the magnitude of current that the p-n junction typically allows through in the reverse biased orientation.

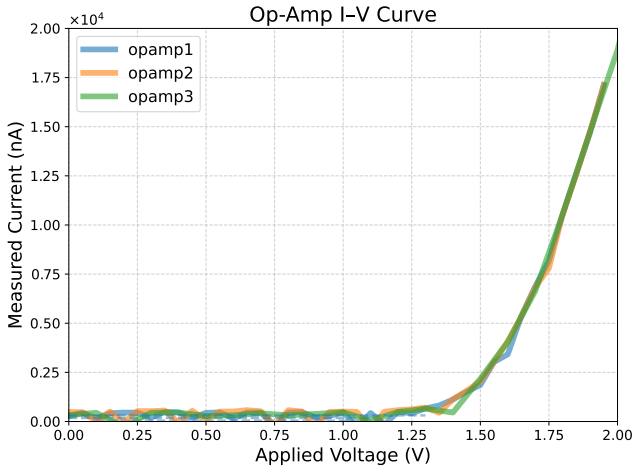

Figure 9: I-V curves for op-amp circuit shown in 5 across voltage sweeps done by using NI DAQ and labview. A clear saturation point is reached before a linear current is output, distinct from transistor output.

Table 1: Data Collection Conditions and Measured Boltzmann Constants for Transistor I-V Measurements. Error in Boltzmann constant calculations is 3% as found in section 2.3.

(a) Data Collection

Temperature (K)	Bias Voltage Range (V)	Data Points	Condition
Cooled Silicon Transistor			
83.2	0–1.2	420	Cooled
86.9	0–1.2	410	Cooled
132.8	0–1.2	395	Cooled
170.4	0–1.0	460	Cooled
186.6	0–1.0	480	Cooled
214.0	0–1.2	430	Cooled
222.7	0–1.2	450	Cooled
238.2	0–1.2	420	Warming
249.4	0–1.2	405	Cooled
274.1	0–1.2	460	Cooling
276.9	0–1.2	400	Warming
Heated Silicon Transistor			
299.1	0–1.0	380	Heated
300.2	0–1.0	375	Heated
304.8	0–1.0	385	Heated
308.8	0–1.0	370	Heated
313.2	0–1.0	390	Heated
318.9	0–1.0	380	Heated
Heated Germanium Transistor			
304.5	0–1.0	380	Heated
306.9	0–1.0	370	Heated
308.3	0–1.0	375	Heated
309.5	0–1.0	365	Heated
310.8	0–1.0	380	Heated
312.2	0–1.0	375	Heated
312.9	0–1.0	370	Heated
315.0	0–1.0	380	Heated
316.1	0–1.0	370	Heated
317.3	0–1.0	375	Heated
318.4	0–1.0	365	Heated

(b) Measured Boltzmann Constants

Temperature (K)	k_{measured} (J/K)	Percent Error (%)	Material
83.21	1.533×10^{-23}	+11.03	Si
86.85	1.584×10^{-23}	+14.73	Si
132.81	2.070×10^{-23}	+49.93	Si
170.39	1.345×10^{-23}	−2.58	Si
186.62	1.125×10^{-23}	−18.52	Si
213.98	1.688×10^{-23}	+22.26	Si
222.71	1.757×10^{-23}	+27.26	Si
238.24	1.894×10^{-24}	−86.28	Si
249.36	1.351×10^{-23}	−2.15	Si
274.11	1.666×10^{-23}	+20.67	Si
276.90	5.558×10^{-24}	−59.74	Si
299.13	1.385×10^{-23}	+0.32	Si
299.65	1.384×10^{-23}	+0.24	Si
300.19	1.385×10^{-23}	+0.32	Si
302.47	1.384×10^{-23}	+0.24	Si
304.53	1.784×10^{-23}	+29.21	Ge
306.94	1.900×10^{-23}	+37.63	Ge
308.26	1.966×10^{-23}	+42.44	Ge
309.49	2.044×10^{-23}	+48.05	Ge
310.76	2.122×10^{-23}	+53.74	Ge
312.16	2.217×10^{-23}	+60.60	Ge
315.02	2.493×10^{-23}	+80.67	Ge
316.11	2.624×10^{-23}	+90.13	Ge

2.3 Measurement Error Analysis

Measurement error in this experiment was dominated by noise that is typical of measurements at very low current levels to examine semiconductor materials. All voltage readings were obtained through the NI DAQ interface with a precision of two decimal digits (0.01 V). Current was measured using the Keithley picoammeter with seven significant digits,and temperature was recorded from the thermocouple sensor with a seven digit digital precision. However, the thermocouple's error is not gated by precision, but rather the cold junction compensation or thermal contact gradient from which we know the uncertainty is approximately $\pm.5\ K$ [4].

For the transistor and diode measurements, the primary sources of random uncertainty come from electrical noise, contact resistance, and DAQ quantization error. Other uncertainties could be possible drift of the picoammeter offsets between the device base and the sensor junction.

The saturation current I_S, ideality factor n, and Boltzmann constant k_B can have their errors calculated in relation to equation 1

$$I = I_S\Big(e^{qV/(nk_\mathrm{B}T)} - 1\Big)$$

After regression on $\ln I$ versus V, the slope m and intercept b become [5]:

$$m = \frac{q}{nk_\mathrm{B}T}, \qquad b = \ln I_S$$

Uncertainties in V, I, and T propagate with

$$\left(\frac{\delta m}{m}\right)^2 = \left(\frac{\delta V}{\Delta V}\right)^2 + \left(\frac{\delta(\ln I)}{\Delta(\ln I)}\right)^2 + \left(\frac{\delta T}{T}\right)^2$$

We can use $\delta(\ln I) \approx \delta I/I$, and reason that the relative contribution of the picoammeter uncertainty is small ($\sim 10^{-7}$ fractional), while the DAQ voltage step size of 0.01 V dominates the error [3].

Propagating k_B gives

$$\frac{\delta k_\mathrm{B}}{k_\mathrm{B}} = \sqrt{\left(\frac{\delta m}{m}\right)^2 + \left(\frac{\delta T}{T}\right)^2}$$

Plugging everything in with $\delta V = 0.01$ V, $\delta I/I \sim 10^{-7}$, and $\delta T = 2 \times 10^{-2}$ K, the total fractional uncertainty in k_B is approximately 3 %.

3 Data Analysis and Results

3.1 Ebers-Moll Fit

3.1.1 Saturation Current Determination

By utilizing the Ebers-Moll equation and the reasoning present in section 1.2.1, we can calculate the saturation current I_s across all of the runs of the transistors. An example of this fit is shown in 13, where the exponential fit is performed on the central region where the p-region is saturated and not plateauing. The saturation current calculated in this example is $I_S = (4.98 \pm 0.15) \times 10^{-9}\ A$. This can be determined for all of the runs in table 1 and averaged to give an experimental result of

$$(6.070 \pm 2.056) \times 10^9 A$$

We note that this determination had higher error than the determination of Boltzmann's constant because of the error being dominated by the thermal voltage calculation.

3.1.2 Boltzmann's Constant

Using the methodology outline in section 1.2.1, we can fit the Ebers-Moll equation to our experimental data and obtain a value of the Boltzmann constant for every experimental run. This was done for the germanium and silicon transistors. The values of each run are shown in table 1. An example of this fit being performed on transistor data is shown in figure 13, in which a liquid nitrogen cooled transistor I-V curve has been restricted to the current increase regime and k_B has been fit to the region. In this particular example, the value of Boltzmann's constant is determined to be $(1.709 \pm 0.03) \times 10^{-23}\ J/K$.

The determination of k_B for germanium shown in 10 shows a linear uptrend in value with increasing temperature, which is unphysical and suggests that there is some error present. This is explicable by recalling that germanium has a much lower bandgap than silicon, which means that thermal excitations of electrons will cause a much higher current flow.

For the silicon data, shown in figures 11 12, we can see that the calculated Boltzmann constant has much higher variance in the nitrogen cooled experiment vs the resistor heated experiment. This can be attributed to the more extreme temperature achieved by the nitrogen and error in the thermocouple.

Finally, taking all of our data in table 1, our calculated

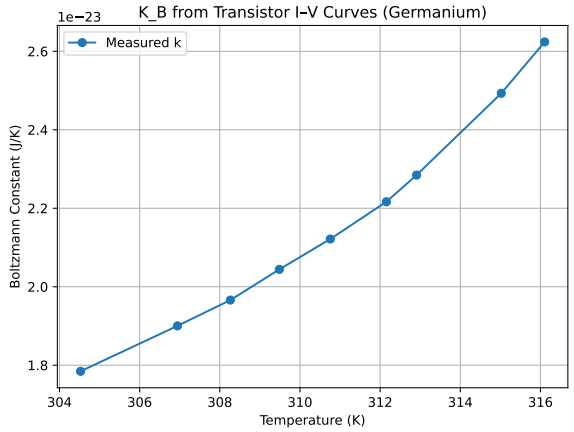

Figure 10: Determination of Boltzmann constants using germanium transistor and equation 1 across experimental I-V runs with a power resistor heating the transistor holding plate. Boltzmann constant value seems to increase nonlinearly with temperature, suggesting that there is a source of error in the data that is being compounded at higher temperature.

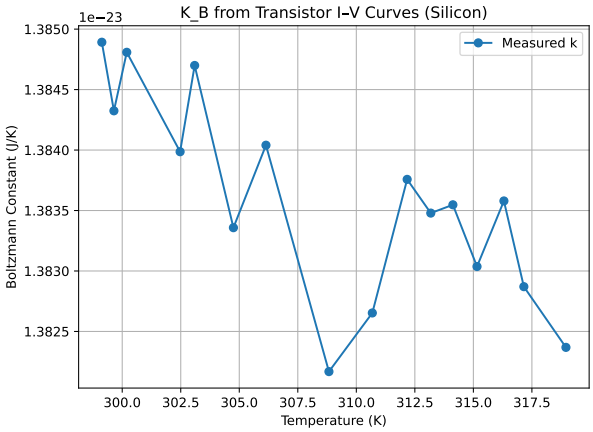

Figure 11: Determination of Boltzmann constants using silicon transistor and equation 1 across experimental I-V runs with a power resistor heating the transistor holding plate. Variance of this dataset is much lower than those of the germanium trials 10 and liquid nitrogen cooled silicon trials 12.

value for the Bolztmann constant is

$$k_B = (1.385 \pm 0.042) \times 10^{-23}\ J/K$$

3.2 Diode Current Leakage

With our three runs of diode data taken with the setup in figure 4 and shown in 8, we can apply the avalanche 5 and Zener 4 fits discussed in section 1.2.5. The fit to the avalanche equation is shown in figure 14 and the fit to the Zener equation is shown in figure 15. The avalanche fit tells us $V_{BR} = 3.3 \pm 0.05V$ while the Zener fit tells us $V_{BR} = 3.71 \pm 0.05\ V$. Visually, it is very clear that the Zener fit does not describe the data very well, while the avalanche fit accounts for more of the behavior of the diode current leakage. This is further exemplified with the higher R^2 values for the avalanche fit, where $R^2(Avalanche) = 0.8727, R^2(Zener) = 0.5632$. From these values, we can determine that in this regime, most of the current is a result of electric potential leakage through the semiconductor rather than the tunneling electrons through the barrier.

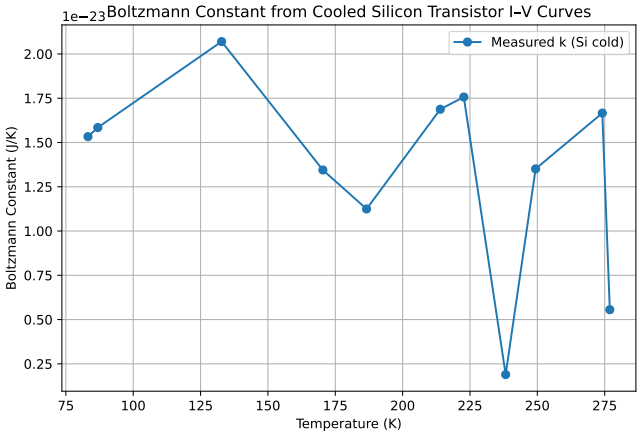

Figure 12: Determination of Boltzmann constants using silicon transistor and equation 1 across experimental I-V runs involving a liquid nitrogen cooled silicon transistor. Variance is significantly higher than those of the heated trials 11, potentially due to noise being amplified with colder temperatures.

3.3 Op-Amp Ebers-Moll Fit

The fit of op-amp I-V characteristics for the circuit in figure 5 across the three expeirmental runs is shown in

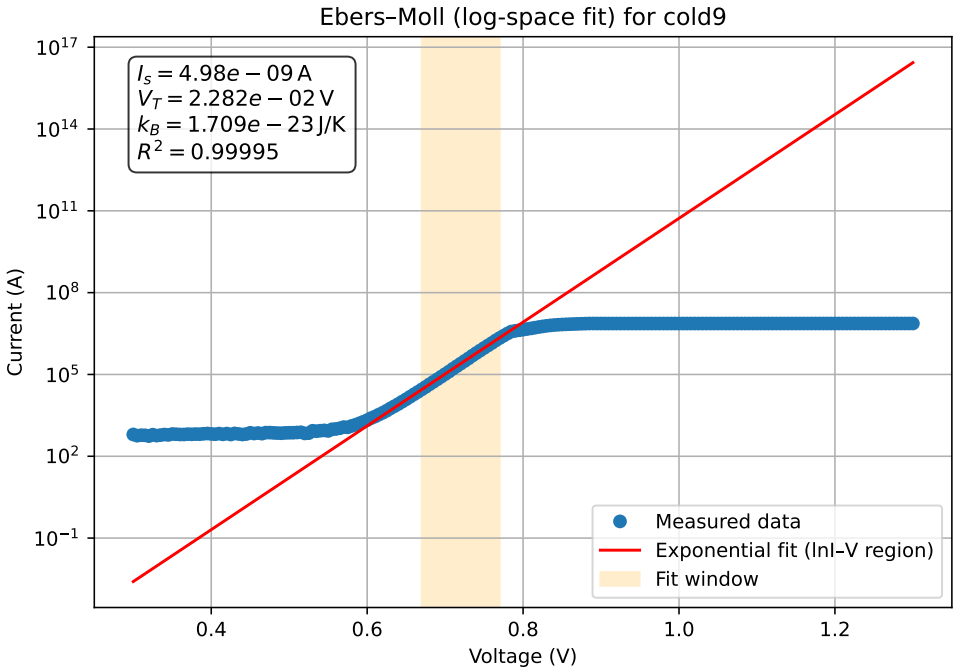

Figure 13: Example of a single Ebers-Moll equation fit onto transistor I-V data. This experimental run utilized a liquid nitrogen cooled silicon transistor. Results for this run show that the Ebers-Moll equation accounted very well for the current behavior after restricting to the region in between the saturation current and plateau. The value of k_B obtained from this result is $(1.709 \pm 0.03) \times 10^{-23}$ J/K and the value of $I_S = (4.988 \pm 0.15) \times 10^{-9}$ A.

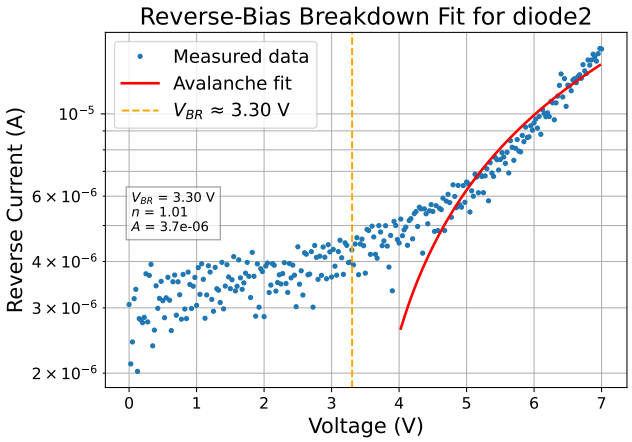

Figure 14: Fit of the avalance equation 5 onto LED current leakage data. In this regime, we can see that the avalanche fit is a reasonable model for the current leakage when there is a significant amount of current. This suggests a better explanation for the current than the results of 15.

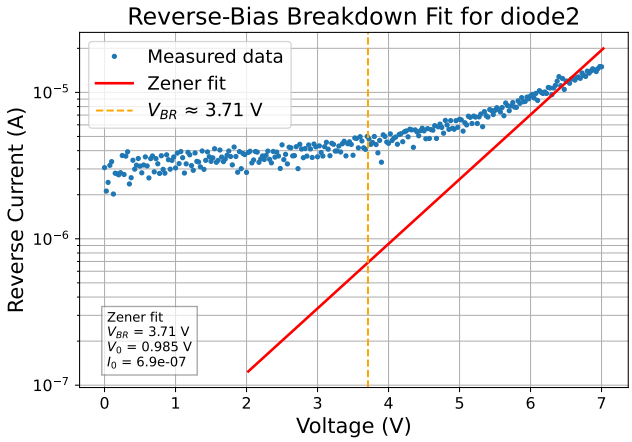

Figure 15: Fit of the Zener equation 4 onto LED current leakage data. In this regime, we can see that the Zener fit does not capture the correct behavior for the breakdown characteristics of the LED, suggesting that the quantum tunneling of electrons is not sufficient to describe this current.

figure 16. The data shows that the saturation current of the op-amp components is $(1.55 \pm 0.047) \times 10^{-9} A$, and the calculated ideality factors are quite high. This indicates lots of noise in the data, which can be seen around the noise floor at the beginning of each curve, with large oscillations in the output. This shows that the input junctions of the op-amp have small leakage current but a strong exponential response in the early saturation regime, before flattening out into the lienar scaling that was discussed in section 1.2.6.

4 Summary and Conclusions

4.1 Boltzmann's Constant

From the Ebers-Moll fits applied to the silicon and germanium transistor I-V curves, we experimentally determined value of the Boltzmann constant was found to be

$$k_B = (1.385 \pm 0.042) \times 10^{-23} \text{ J/K}$$

which is in very close agreement with the accepted value of $k_{B,\text{true}} = 1.380649 \times 10^{-23}$ J/K [2]. This agreement within uncertainty shows the Ebers-Moll model to be valid and gives us valuable insight into one of the fundamental constants on physics. Deviations from each individual experiment run are shown in table 1, and we note that individual trials varied quite significantly from the correct result, even though all were in the correct order of magnitude. However, the average of all of the recorded data did indeed lead us very close to the accepted answer.

4.2 Saturation Current

From the Ebers–Moll fit performed on both of the transistors, the average saturation current was determined to be:

$$I_s = (6.07 \pm 2.06) \times 10^{-9} \text{ A}$$

Which is consistent with the expected order of magnitude for silicon-based bipolar junction transistors. Leakage and diffusion currents typically fall within the nanoamp range. This I_s shows the reverse-bias carrier current through the base–emitter junction, which is what determines the scale factor of the exponential current relation in Ebers-Moll.

The uncertainty is large compared to the Boltzmann constant determination, and can be attributed in part to the sensitivity of the exponential fit to the linear region that the fit is done over. This is because small deviations in slope or measurement noise in the low-current regime can introduce large deviations in the intercept and final calculation. Variations in temperature and other noise between runs akso introduces some systematic errors that propagated through the thermal voltage value.

4.3 Diode results

From the reverse-bias I-V measurements of the LED, we fitted both the avalanche and Zener breakdown models to see which mechanism best describes the observed current leakage. The fitted parameters gave breakdown voltages of

$$V_{\text{BR, Avalanche}} = 3.30 \pm 0.05 \text{ V} \qquad V_{\text{BR, Zener}} = 3.71 \pm 0.05 \text{ V}$$

The avalanche fit gave a coefficient of determination $R^2 = 0.8727$ and the Zener fit gave $R^2 = 0.5632$. This clearly indicates that the avalanche model provides a much better description of the breakdown behavior. Physically, this suggests that the reverse current in the LED is due to impact ionization rather than quantum tunneling through the p-region's potential barrier. In other words, charge carriers get kinetic energy from the electric field to create additional electron–hole pairs through collisions more than they tunnel across the potential barrier in this regime

4.4 Op-Amp Results

The Ebers-Moll fit on the op-amp I-V data gave us:

$$I_s = (1.55 \pm 0.047) \times 10^{-9} \text{ A}$$

with ideality factors, n, of between $n = 7.6$ and $n = 8.1$ across the three experimental runs. These high values of n deviate significantly from the ideal diode expectation ($n \approx 1$), which shows that the junctions inside the op-amp are very far from ideal diodes. This is possibly due to the complex junctions inside the op-amp exhibiting behavior that does not perfectly match singular diodes.

The I_s value being on the order of nanoamperes is consistent with expected input leakage currents of op-amps in general, confirming that only a very small reverse saturation current flows through the input transistor junc-

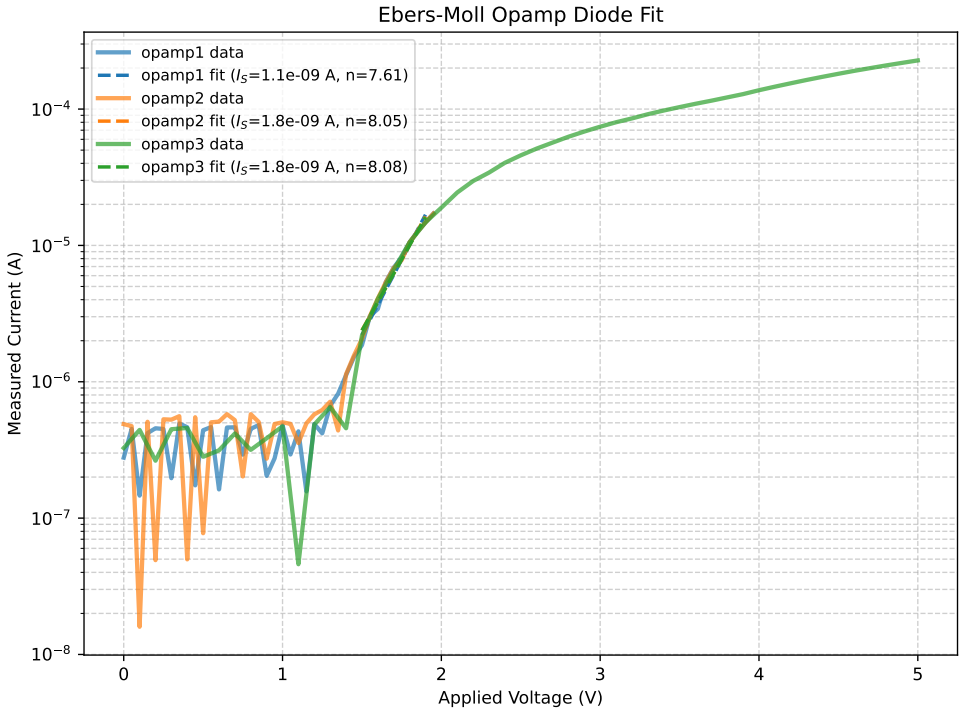

Figure 16: Ebers-Moll diode fit for op-amp I-V curve data using equation 1. The fit shows low ideality and an I_s on the order of 10^{-9} A. Data was taken and fitted across 3 runs with the same op-amp. Low ideality can be seen, with the ideality factor n being much higher than unity, meaning there is significant noise in these measurements, or a departure from ideal op-amp characteristics within this component specifically.

tions. Meanwhile, the large ideality factors and the noisy low-voltage region of the curves suggest that measurement noise and internal biasing currents within the op-amp have a high impact on what we observe. This can be seen in the oscillations near the current noise floor, which imply that thermal noise and input offset voltages of the op-amp alter the signal drastically at low bias. Once the voltage exceeds about 1.5 V, the exponential increase in current becomes more consistent, which is another result that supports the validity of the Ebers–Moll model.

4.5 Conclusion

In this experiment, we investigated the behavior of semiconductor materials and important electrical components that rely on them. such as bipolar junction transistors, diodes, and operational amplifiers. We varied temperature and voltage bias conditions of transistors, and used the Ebers–Moll model to analyze exponential regions of current output. This allowed us to determine the Boltzmann constant and the saturation current across multiple trials. We went beyond the lab manual and characterized reverse-bias breakdown in LEDs by fitting both the avalanche and Zener equations, and we also analyzed the difference between ideal and non-ideal diode behavior by using the op-amp input junctions to test the Ebers-Moll model.

The averaged result of Boltzmann constant for our experimental trials was $k_B = (1.385 \pm 0.042) \times 10^{-23}$ J/K,, which agrees very strongly with the accepted value of 1.38×10^{-23} J/K within experimental uncertainty. The averaged saturation current for the transistors we used was found to be $(6.07 \pm 2.06) \times 10^{-9}$ A, consistent with expected nanoamp-scale leakage in forward-biased silicon junctions. For the LED reverse-bias tests, the avalanche model explained more of the observed results ($R^2 \approx 0.87$) compared to the Zener model, which confirms that impact ionization is more influential than tunneling for the breakdown at $V_{\mathrm{BR}} \approx 3.3$ V. Finally, the op-amp junctions showed saturation currents near 10^{-9} A but we found very large ideality factors ($n \approx 8$) in our data, which could be due to the junction structure inside op-amps as well as measurement noise. Our results verify many of the well-known properties of semiconductors and show good

agreement with previous results. The ability to use semiconductor properties to calculate a fundmanetal constant of physics as well as their importance in modern electronics has made this a worthwhile experiment and a valuable exercise in independent laboratory procedure.

4.6 Future Work Considerations

Future iterations of this experiment could consider doing more careful calibration of the picoammeter to better quantify the error, using higher voltages on the diode circuit and op-amp rails to look at the very large V regime, as well as cooling the germanium transistor in liquid nitrogen like the silicon transistor was cooled.

Acknowledgements: Thank you to my partner, Adin Viera, and to the lab TAs, Joshua and Oorie.

References

[1] dpardo. *741 Schematic Op Amp Circuit*. URL: https://www.circuitlab.com/circuit/85jw9juhqdye/741-schematic-op-amp-circuit/.

[2] Paul Horowitz and Winfield. Hill. *The art of electronics /*. 2nd ed. Cambridge : Cambridge University Press, 1989.

[3] National Instruments. *NI USB-6346 Specifications*. URL: https://mm.digikey.com/Volume0/opasdata/d220001/medias/docus/4820/USB-6346_Spec.pdf?_gl=1*1sir3le*_up*MQ..*_gs*MQ..&gclid=CjwKCAiAwqHIBhAEEiwAx9cTeUjZ1cofdUSXjRdHOon_eCRpSulN64BVD6polk4JKVCCpsLSkhUchxoCAxIQAvD_BwE&gclsrc=aw.ds&gbraid=0AAAADrbLljDA-ceRcKSer-xjjdymho_o.

[4] Texas Instruments. *Thermocouple, Cold-Junction Compensation— Analog Approach*. URL: https://www.ti.com/lit/an/sloa204/sloa204.pdf?utm_source=chatgpt.com&ts=1762718928508&ref_url=https%253A%252F%252Fchatgpt.com%252F.

[5] Inc. Keithley Instruments. *Model 6485 Picoammeter Instruction Manual*. Document No. 6485-901-01 Rev. A. Keithley Instruments, Inc. Cleveland, Ohio, U.S.A., Nov. 2001. URL: https://uhv.cheme.cmu.edu/manuals/picoammeter-6485.pdf.

[6] Leonard M. Krugman. *Radiation Detection and Measurement*. 1st ed. New York: RIDER, 1954. URL: http://www.tubebooks.org/books/krugman_transistors.pdf.

[7] Chemistry Libretexts. "2.4: Semiconductors". In: (). URL: https://chem.libretexts.org/Bookshelves/Analytical_Chemistry/Instrumental_Analysis_(LibreTexts)/02%3A_Electrical_Components_and_Circuits/2.04%3A_Semiconductors.

[8] Chemistry Libretexts. *5: LED (Light Emitting Diodes)*. URL: https://chem.libretexts.org/Courses/University_of_Arkansas_Little_Rock/IOST_Library/07%3A_Electronics_Book/2%3A_Electronic_Components/05%3A_LED_(Light_Emitting_Diodes).

[9] Engineering Libretexts. "4.5: Ebers-Moll Model". In: (). URL: https://eng.libretexts.org/Bookshelves/Electrical_Engineering/Electronics/Semiconductor_Devices_-_Theory_and_Application_(Fiore)/04%3A_Bipolar_Junction_Transistors_(BJTs)/4.5%3A_Ebers-Moll_Model.

[10] Engineering Libretexts. *8.5: Thermoelectric Effects*. URL: https://eng.libretexts.org/Bookshelves/Electrical_Engineering/Electro-Optics/Direct_Energy_(Mitofsky)/08%3A_Thermoelectrics/8.05%3A_Thermoelectric_Effects.

[11] L. et al. Łukasiak. "History of Semiconductors". In: *Journal of Telecommunications and Information Technology* (). URL: https://djena.engineering.cornell.edu/hws/history_of_semiconductors.pdf.

[12] Adrian C. Melissinos and Jim Napolitano. *Experiments in Modern Physics*. 2nd. San Diego: Academic Press, 2003. ISBN: 978-0-12-489851-6.

[13] Arduino Scuola. *How to use BJTs*. URL: https://projecthub.arduino.cc/Arduino_Scuola/how-to-use-bjts-a4ef5a.

[14] STMicroelectronics. *BUL216 High Voltage Fast-Switching NPN Power Transistor*. URL: https://web2.ph.utexas.edu/~phy353l/SemiconductorPhysics/TO220DataSheet.pdf.